NEUROSCIENCE

Identification of an ionic mechanism for ERα-mediated rapid excitation in neurons

Meng Yu[1]†, Na Yin[1]†, Bing Feng[2], Peiyu Gao[2], Kaifan Yu[1], Hesong Liu[1], Hailan Liu[1], Yongxiang Li[1], Olivia Z. Ginnard[1], Kristine M. Conde[1], Mengjie Wang[1], Xing Fang[1], Longlong Tu[1], Jonathan C. Bean[1], Qingzhuo Liu[1], Yue Deng[1], Yuxue Yang[1], Junying Han[1], Sanika V. Jossy[1], Megan L. Burt[1], Huey Zhong Wong[1], Yongjie Yang[1], Benjamin R. Arenkiel[3], Yang He[3], Shaodong Guo[4], Pierre Gourdy[5], Jean-Francois Arnal[6], Francoise Lenfant[6], Zhao Wang[7,8], Chunmei Wang[1], Yanlin He[2]*, Yong Xu[1,8,9]*

The major female ovarian hormone, 17β-estradiol (E_2), can alter neuronal excitability within milliseconds to regulate a variety of physiological processes. Estrogen receptor-α (ERα), classically known as a nuclear receptor, exists as a membrane-bound receptor to mediate this rapid action of E_2, but the ionic mechanisms remain unclear. Here, we show that a membrane channel protein, chloride intracellular channel protein-1 (Clic1), can physically interact with ERα with a preference to the membrane-bound ERα. Clic1-mediated currents can be enhanced by E_2 and reduced by its depletion. In addition, Clic1 currents are required to mediate the E_2-induced rapid excitations in multiple brain ERα populations. Further, genetic disruption of Clic1 in hypothalamic ERα neurons blunts the regulations of E_2 on female body weight balance. In conclusion, we identified the Clic1 chloride channel as a key mediator for E_2-induced rapid neuronal excitation, which may have a broad impact on multiple neurobiological processes regulated by E_2.

INTRODUCTION

17β-estradiol (E_2), the major female ovarian hormone, can act in the brain to regulate a variety of physiological processes, including female fertility (*1*, *2*), sexual behaviors (*3*), mood (*4*), reward (*5*), stress response (*6*), cognition (*7*), cardiovascular activities (*8*), and metabolic homeostasis (*9*–*11*). Many of these E_2 functions are mediated by one of the estrogen receptors (ERs), namely, estrogen receptor-α (ERα). As a classic nuclear receptor, ERα can translocate to the nucleus, upon stimulation by E_2, to directly bind to the estrogen response elements (EREs) on the target genes and regulate gene transcription. Nuclear ERα can also form complexes with other nuclear receptors or transcription factors, which regulates gene transcription in an ERE-independent manner (*9*). Recent evidence indicates that ERα is a potent RNA binding protein that regulates splicing and translation of various mRNAs (*12*). Notably, a subpopulation of ERα protein is concentrated on the cell membrane (*13*), where it initiates rapid signaling pathways (*14*–*16*). These E_2-initiated rapid actions are indispensable for multiple female biological processes, e.g., sexual behavior (*17*), fertility (*18*), energy, and glucose balance (*19*, *20*).

We and others have shown that E_2 can also rapidly excite neurons over a period of milliseconds (*13*, *21*–*26*). These rapid electric events are independent of nuclear receptor signaling or RNA binding function, which would take minutes or hours to occur. An open and critical question in the field is how E_2 regulates neuron excitability in such a short time frame. While other ERs, e.g., the G protein–coupled estrogen receptor (GPER) (*27*) and ERβ (*9*, *28*), may contribute to the rapid E_2 actions, we have demonstrated that genetic deletion of ERα alone is sufficient to abolish E_2-induced excitation in neurons in several brain regions we tested (*21*–*24*, *29*). These results indicate that ERα mediates rapid estrogen-induced excitation in neurons, and we further hypothesize that ERα does so by physically interacting with membrane proteins that allow rapid alterations in neuronal excitability.

In the current study, we initiated a search for ERα-interacting membrane proteins and identified a chloride channel protein, chloride intracellular channel protein-1 (Clic1), which can physically interact with ERα. Clic1 exists as both soluble and integral membrane forms in cells and has been implicated in the regulation of neuronal excitability and intracellular redox balance (*30*). We further examined Clic1 currents in multiple brain ERα populations and their roles in mediating E_2-induced rapid excitations in neurons. Last, we assessed the functional relevance of Clic1 in hypothalamic ERα neurons in the context of female energy balance.

RESULTS

ERα interacts with Clic1

We used a BioID-MS approach (*31*) to identify a total of 553 proteins that interact with the wild-type (WT) ERα protein (Fig. 1, A and B; fig. S1; and table S1). Among these proteins, 98 are known to be membrane proteins. In particular, we noted Clic1, a chloride channel that can localize to the plasma membrane to regulate chloride permeability cross the cell membrane (*32*, *33*). Next, we used the co-immunoprecipitation approach to confirm the interaction of the recombinant ERα and Clic1 proteins (Fig. 1C). Similarly, in human

[1]USDA/ARS Children's Nutrition Research Center, Department of Pediatrics, Baylor College of Medicine, One Baylor Plaza, Houston, TX 77030, USA. [2]Brain Glycemic and Metabolism Control Department, Pennington Biomedical Research Center, Louisiana State University, Baton Rouge, Louisiana, USA. [3]Department of Molecular and Human Genetics, Baylor College of Medicine, Houston, TX 77030, USA. [4]Department of Nutrition, College of Agriculture and Life Sciences, Texas A&M University, College Station, TX 77843, USA. [5]I2MC, Inserm U1297, CHU de Toulouse and Université de Toulouse III, Toulouse, France. [6]I2MC, Inserm U1048, CHU de Toulouse and Université de Toulouse III, Toulouse, France. [7]Department of Biochemistry and Molecular Pharmacology, Baylor College of Medicine, Houston, TX 77030, USA. [8]Department of Molecular and Cellular Biology, Baylor College of Medicine, Houston, TX 77030, USA. [9]Department of Medicine, Baylor College of Medicine, Houston, TX 77030, USA.
*Corresponding author. Email: yongx@bcm.edu (Y.X.); yanlin.he@pbrc.edu (Y.H.)
†These authors contributed equally to this work.

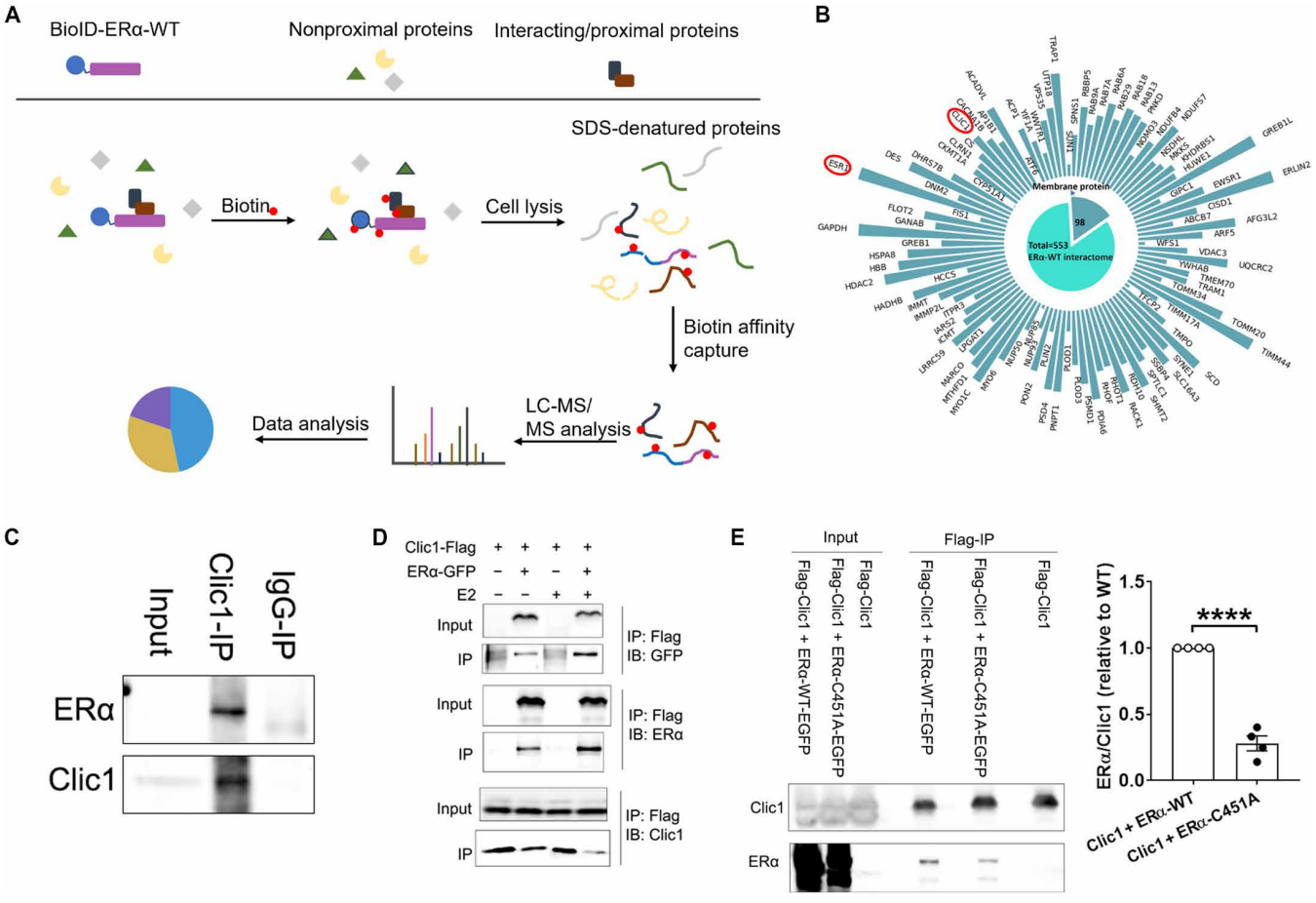

Fig. 1. ERα interacts with Clic1. (**A**) BioID to screen for ERα-interacting proteins. (**B**) ERα-interacting membrane proteins, with ERα (encoded by the ESR1 gene) and CLIC1 highlighted by the red circles. ERα interactors are classified on the basis of their subcellular localization. The same BioID-MS were performed in two independent biological experiments. (**C**) Co-immunoprecipitation showing the interaction of recombinant human ERα and Clic1 proteins in the test tube. The same results were repeated in three independent biological experiments. (**D**) Co-immunoprecipitation showing the interaction of overexpressed human ERα-GFP and Clic1-Flag proteins in HEK293T cells. Cells coexpressing Clic1-Flag and ERα-EGFP were treated with or without E_2 for 30 min. The Clic1-Flag protein complex was then pulled down using Flag-M2 magnetic beads. Clic1 and ERα were identified by Western blotting. The same results were repeated in three independent biological experiments. (**E**) Co-immunoprecipitation showing the interaction of ERα-WT or ERα-C451A and Clic1 proteins in HEK293 cells. Cells coexpressing Clic1-Flag and ERα-WT-EGFP (or ERα-C451A-EGFP) were subjected to immunoprecipitation with Flag-M2 beads. Identification of Clic1 and ERα in the immunoprecipitation samples was performed by Western blotting. Data are quantified from four independent biological experiments. Data are presented as means ± SEM. ****$P < 0.0001$ in two-sided unpaired *t* test. IP, immunoprecipitation. IgG, immunoglobulin G; WT, wild type; LC-MS, liquid chromatography tandem mass spectrometry.

embryonic kidney (HEK) 293T cells cotransfected with ERα–green fluorescent protein (GFP) and Clic1-Flag constructs, we detected the interaction of ERα and Clic1, which was further enhanced by E_2 treatment (Fig. 1D). We and others (*34*, *35*) reported that the point mutation of the palmitoylation site of ERα (ERα-C451A) specifically reduces the membrane-bound ERα abundance, while the transcriptional activity of ERα is preserved. Here, we further demonstrated that the interaction between Clic1 and the ERα-C451A proteins was significantly reduced compared to the interaction between Clic1 and WT ERα proteins (Fig. 1E), indicating that Clic1 preferentially interacts with the membrane-bound ERα.

E_2-ERα signaling enhances Clic1-mediated currents

We have previously demonstrated that E_2 can rapidly excite ERα-expressing populations in the ventrolateral subdivision of ventromedial hypothalamic nucleus (vlVMH) and the arcuate nucleus (ARH) (*21*). The E_2-induced rapid excitation in both these populations can be abolished by the ERα-C451A mutation (*21*). Here, we assessed effects of E_2-ERα signaling on Clic1-mediated currents in ERα^{vlVMH} neurons. To this end, brain slices containing the vlVMH were prepared from female ERα-ZsGreen mice (*36*) in which ERα-expressing neurons were labeled by the ZsGreen fluorescence protein (fig. S2A) and subjected to electrophysiological recordings. Using a published voltage-clamp protocol (*37*), we detected robust voltage-dependent currents in ERα^{vlVMH} neurons (Fig. 2A). Notably, these currents were inward at the negative voltages but became outward at the positive voltages (Fig. 2A). A Clic1 inhibitor, indanyloxyacetic acid 94 (IAA-94), significantly reduced the currents, and the subtractions were calculated as IAA-94–sensitive currents (Fig. 2A). We then repeated the same voltage-clamp protocol with the free [Cl^-] intracellular pipette solution and found that the IAA-94–sensitive inward currents were diminished, while the outward currents were also

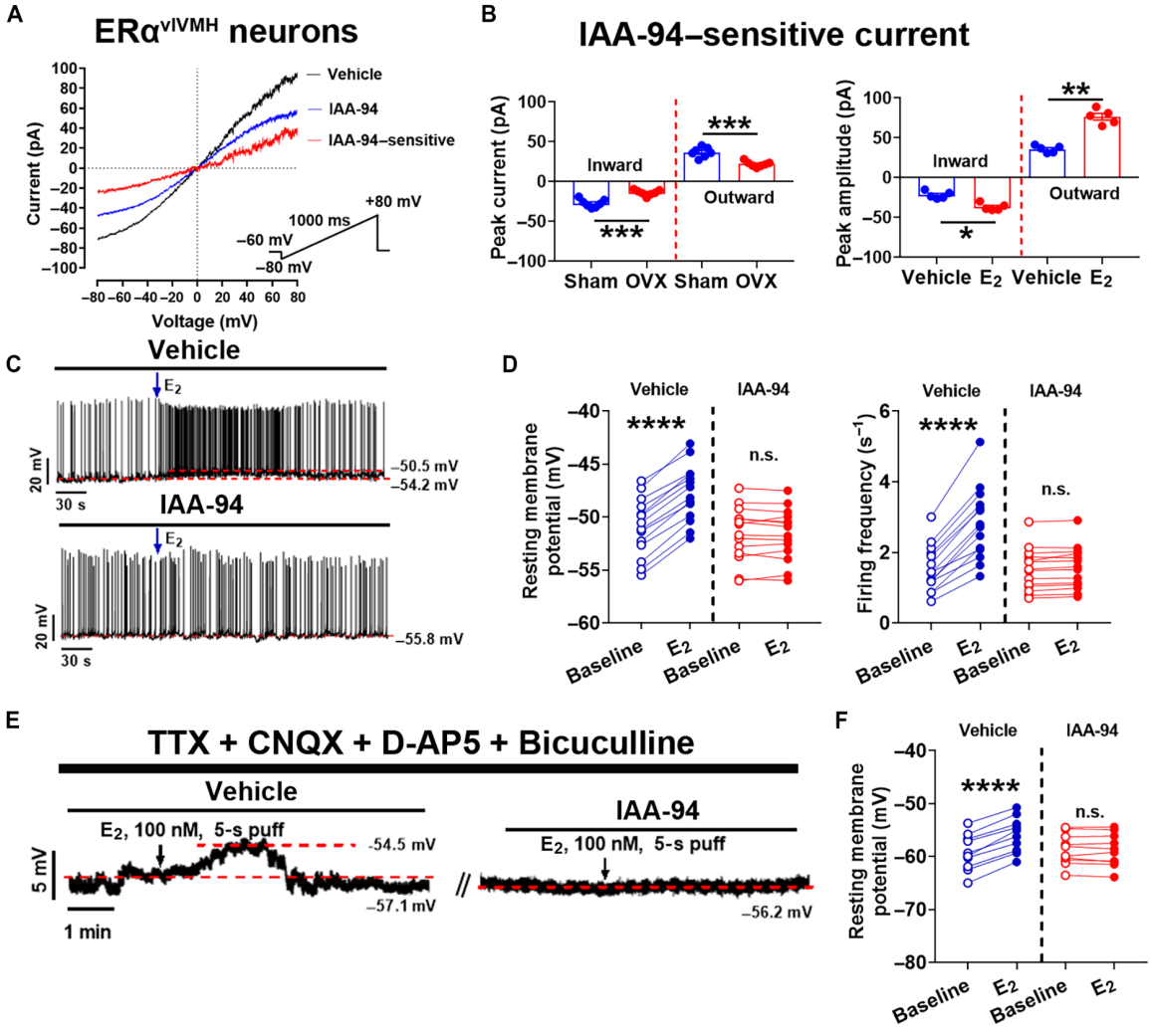

Fig. 2. Clic1 mediates E_2-induced rapid excitation in ERα^{vlVMH} neurons. (**A**) Voltage-dependent currents in an ERα^{vlVMH} neuron in the absence (black) and presence (blue) of IAA-94, and the subtraction (red) as the IAA-94–sensitive current. (**B**) Peak inward and outward IAA-94-senstive currents in ERα^{vlVMH} neurons. Left: Sham versus OVX control female mice; right: vehicle versus E_2-treated (100 nM) brain slices from gonad-intact control female mice. $N = 5$ or 7 neurons from three mice per group. $^*P < 0.05$, $^{**}P < 0.01$, and $^{***}P < 0.001$ in two-sided unpaired *t* tests. (**C**) Traces of the current clamp recording from ERα^{vlVMH} neurons in response to E_2 treatment (100 nM) in the presence or absence of IAA-94. (**D**) Resting membrane potential (left) and firing frequency (right) of ERα^{vlVMH} neurons ($N = 14$) at the baseline and after E_2 treatment (100 nM) in the presence or absence of IAA-94. $^{****}P < 0.0001$ in two-way analysis of variance (ANOVA) analysis followed by Šídák comparisons. (**E**) Traces of the current clamp recording from ERα^{vlVMH} neurons in response to E_2 treatment (100 nM) in the presence or absence of IAA-94, with TTX, CNQX, D-AP5, and bicuculline in the perfusion buffer. (**F**) Resting membrane potential of ERα^{vlVMH} neurons ($N = 10$) at the baseline and after E_2 treatment (100 nM) in the presence or absence of IAA-94, with TTX, CNQX, D-AP5, and bicuculline in the perfusion buffer. $^{****}P < 0.0001$ in two-way ANOVA analysis followed by Šídák comparisons. Data are presented as means ± SEM with individual data points. n.s., not significant.

significantly reduced (fig. S2B). We then compared sham female ERα-ZsGreen mice (with intact gonads) and ovariectomized (OVX) female ERα-ZsGreen mice with ovarian hormones surgically depleted. Compared to the robust IAA-94–sensitive currents in ERα^{vlVMH} neurons from sham female mice, ERα^{vlVMH} neurons from OVX females showed significantly reduced currents (Fig. 2B, left). We failed to detect significant changes in Clic1 mRNAs in the mediobasal hypothalamus from sham versus OVX female mice (fig. S2C), although we could not fully exclude the possibility that OVX may influence Clic1 protein levels. Further, we treated brain slices from gonad-intact ERα-ZsGreen female mice with vehicle or E_2 and found that E_2 treatment significantly increased Clic1 currents in ERα^{vlVMH} neurons (Fig. 2B, right). Together, these results indicate that E_2-ERα signaling can enhance Clic1 currents in ERα^{vlVMH} neurons. To examine the potential role of Clic1 in ERα-expressing neurons in males, we repeated the same recordings to measure IAA-94–sensitive Clic1 currents in ERα^{vlVMH} neurons from ERα-ZsGreen male mice. We observed similar IAA-94–sensitive currents in male ERα^{vlVMH} neurons, but these male currents were significantly smaller than those from sham females; in addition, the castration in males did not alter these currents (fig. S2D).

Clic1 mediates rapid neuronal excitation induced by E_2-ERα signaling

We then sought to determine whether Clic1 currents are required to mediate rapid neuronal excitation. Using electrophysiology, we

showed that E_2 (10, 100, and 1000 nM) depolarized the resting membrane potential of ERα^{vlVMH} neurons and increased their firing frequency (fig. S3, A and B). Notably, effects of 100 nM E_2 were significantly stronger than 10 nM E_2 and comparable to those of 1000 nM E_2 (fig. S3, C and D). Further, we showed that 100 nM E_2 significantly reduced input resistance (fig. S3E), suggesting the opening of ion channels. In addition, neither a GPER antagonist (G15) not an ERβ antagonist (PHTPP) affected E_2-induced activation in these neurons, indicating that these E_2 effects in ERα^{vlVMH} neurons are independent of GPER and ERβ (fig. S3F). Notably, ERα is also reported to interact with the voltage-dependent anion channel 1 (VDAC1), which primarily locates at the outer mitochondrial membrane (*38*). Here, we showed that in the presence of a VDAC1 inhibitor, VBIT-12 (*39*), 100 nM E_2 induced comparable activation of ERα^{vlVMH} neurons (fig. S3F), indicating that VDAC1 is not involved in this effect.

Perfusion of the Clic1 inhibitor, IAA-94, abolished the depolarization and increased firing frequency induced by 100 nM E_2 (Fig. 2, C and D). To exclude the possibility that E_2 may excite ERα^{vlVMH} neurons via a presynaptic mechanism, we repeated these recordings in the presence of tetrodotoxin (TTX) and a cocktail of synaptic inhibitors (CNQX, D-AP5, and bicuculline). Under this condition, 100 nM E_2 still rapidly depolarized ERα^{vlVMH} neurons, and these effects were abolished by IAA-94 (Fig. 2, E and F). Because the AMP-activated protein kinase (AMPK) has been implicated to mediate actions of E_2 on hypothalamic neurons, we further tested effects of an AMPK activator, A769662 (*40*), on ERα^{vlVMH} neurons. A769662 significantly activated ERα^{vlVMH} neurons, an effect that was significantly attenuated by pretreatment of IAA-94 (fig. S3, G and H). These results further support the notion that Clic1 currents mediate E_2 actions to excite these neurons.

Because IAA-94 may have nonspecific effects other than inhibiting Clic1, we sought to further confirm the role of Clic1 using a CRISPR-mediated genetic deletion approach. To this end, we designed and validated two single guide RNAs (sgRNAs) that induce indel mutations in exon 2 and exon 5 of mouse *Clic1* gene and constructed these sgRNAs into an Adeno-associated virus (AAV) vector followed by Cre-dependent FLEX-tdTOMATO sequence (fig. S4A). Here, female ERα-Cre mice received stereotaxic injections of AAV-FLEX-saCas9 and AAV-Clic1/sgRNAs-FLEX-tdTOMATO into one side of the vlVMH to disrupt the expression of *Clic1* selectively in vlVMH neurons; as controls, the other side of the vlVMH of the same mice received AAV-FLEX-GFP and AAV-Clic1/sgRNAs-FLEX-tdTOMATO (Fig. 3A). Using single-cell polymerase chain reaction (PCR), we validated the expected DNA editing in the *Clic1* gene in the deletion side (fig. S4, B and C). Ultimately, we validated the loss of Clic1 at the functional level by recording Clic1 currents. While abundant Clic1 currents were detected in ERα^{vlVMH} neurons from the control side, Clic1 currents were significantly reduced in ERα^{vlVMH} neurons from the deletion side (Fig. 3B). E_2 induced rapid excitations in control ERα^{vlVMH} neurons, and these effects were abolished in ERα^{vlVMH} neurons with Clic1 deletion (Fig. 3C).

Clic1 currents exist in other neural populations

We then repeated the same studies in a number of ERα populations in the brain, including ERα^{ARH} neurons and those in the medial amygdala (MeA), the bed nucleus of that stria terminalis (BNST), the lateral hypothalamus (LH), and the pre-optic area of the hypothalamus (POAH). Similarly, we detected IAA-94–sensitive Clic1 currents in all these ERα populations, which were further enhanced by E_2 treatment (Fig. 4, A, D, G, J, and M). E_2 rapidly activated these ERα neurons, in the presence or absence of TTX and the synaptic inhibitors, and IAA-94 effectively abolished these E_2-induced excitations (Fig. 4, B and C, E and F, H and I, K and L, and N and O). Thus, Clic1 is a common ionic mechanism for E_2 to excite ERα neurons in multiple brain regions.

Clic1 in ERα^{vlVMH} and ERα^{ARH} neurons mediates effects of E_2 fluctuations on energy balance in female mice

Because ERα^{vlVMH} neurons and ERα^{ARH} neurons have been reported to mediate estrogenic actions on female energy balance through regulating food intake, physical activity, and/or energy expenditure (*29*, *41*–*45*), we then sought to determine whether Clic1 currents in these neurons are functionally involved in these estrogenic actions. To this end, female ERα-Cre mice received stereotaxic injections of AAV-FLEX-saCas9 and AAV-Clic1/sgRNAs-FLEX-tdTOMATO into both sides of the mediobasal hypothalamus that contains the vlVMH and ARH [with a modest contamination to the dorsomedial hypothalamus (DMH)] (Fig. 5A and fig. S5A). As controls, WT female littermates received the same stereotaxic virus injections. These mice all

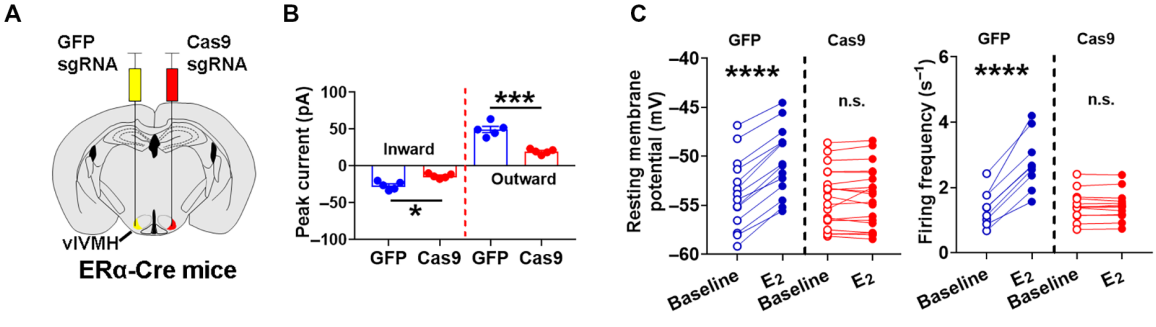

Fig. 3. Deletion of Clic1 blocks E_2-induced rapid excitation in ERα^{vlVMH} neurons. (**A**) An illustration of Clic1 genetic disruption in ERα neurons from one side of the vlVMH and using ERα neurons from the other side of vlVMH as controls. (**B**) Peak inward and outward IAA-94–senstive currents in ERα^{vlVMH} neuron from Clic1 disrupted side (Cas9) versus the control side (GFP). $N = 5$ neurons from three mice per group. $^*P < 0.05$ and $^{***}P < 0.001$ in two-sided unpaired *t* tests. (**C**) Resting membrane potential (left) and firing frequency (right) of ERα^{vlVMH} neurons from Clic1 disrupted side (Cas9; $N = 14$) versus the control side (GFP, $N = 21$) at the baseline and after E_2 treatment (100 nM). $^{****}P < 0.0001$ in two-way ANOVA analysis followed by Šídák comparisons. Note that some neurons did not have spontaneous action potential firing and therefore were not included in the firing frequency analysis. Data are presented as means ± SEM with individual data points.

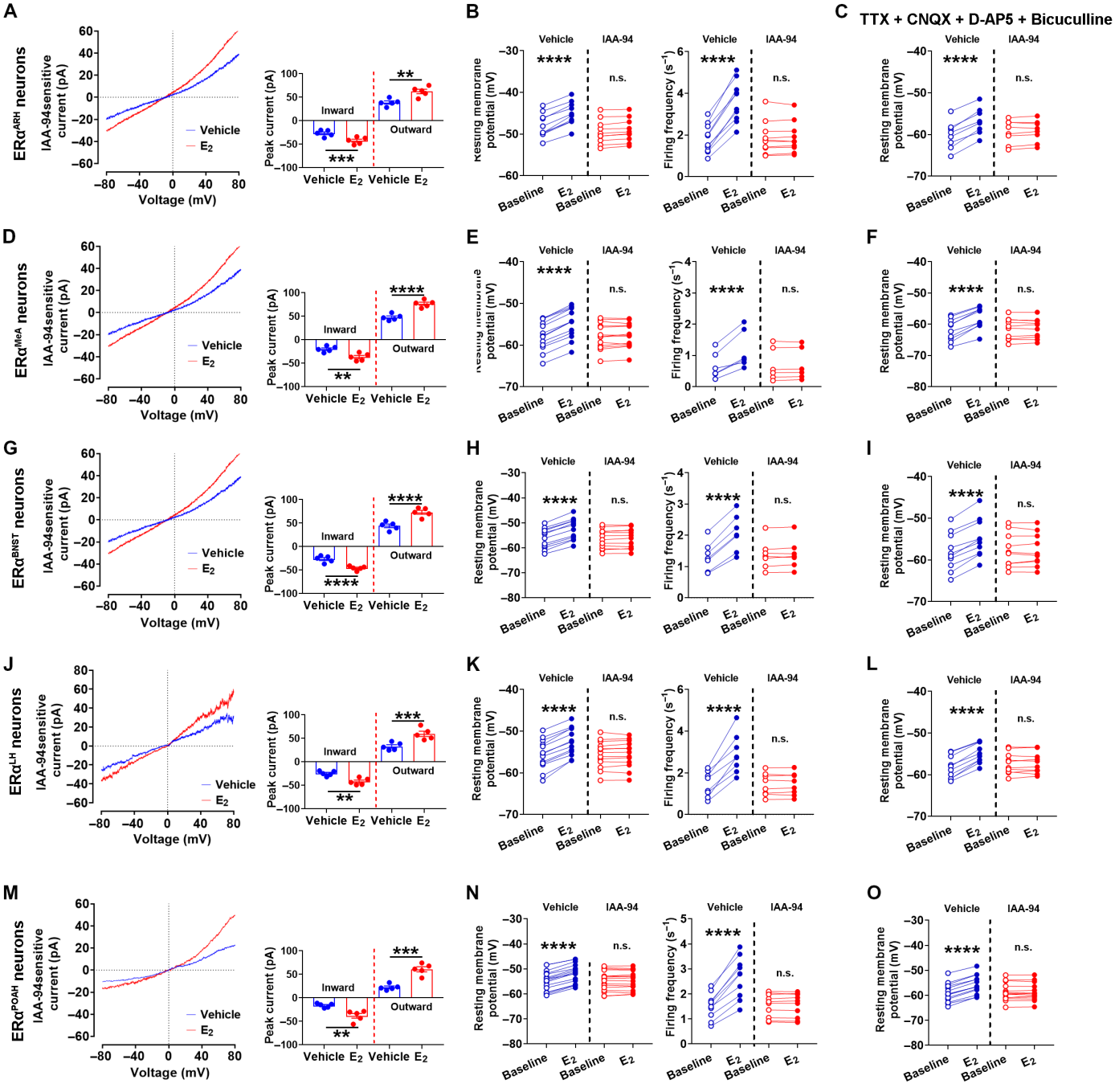

Fig. 4. Clic1 mediates E_2-induced rapid excitation in ERα neurons in the brain. (**A**, **D**, **G**, **J**, and **M**) Left: IAA-94–sensitive current measured in ERα^{ARH} neuron (A), ERα^{MeA} neuron (D), ERα^{BNST} neuron (G), ERα^{LH} neuron (J), and ERα^{POAH} neuron (M) in the absence or presence of E_2 treatment (100 nM). Right: Peak inward and outward IAA-94–sensitive currents measured in the absence or presence of E_2 treatment (100 nM). Data are presented as means ± SEM with individual data points. $N = 5$ neurons from three different mice per group. $^{**}P < 0.01$, $^{***}P < 0.001$, and $^{****}P < 0.0001$ in two-sided unpaired *t* tests. (**B**, **E**, **H**, **K**, and **N**) Resting membrane potential (left) and firing frequency (right) of ERα^{ARH} neurons (B), ERα^{MeA} neurons (E), ERα^{BNST} neurons (H), ERα^{LH} neurons (K), and ERα^{POAH} neurons (N) at the baseline and after E_2 treatment (100 nM) in the presence or absence of IAA-94 (100 μM). Data are presented as individual data points. $^{****}P < 0.0001$ in two-way ANOVA analysis followed by Šídák comparisons. (**C**, **F**, **I**, **L**, and **O**) Resting membrane potential of ERα^{ARH} neurons (C), ERα^{MeA} neurons (F), ERα^{BNST} neurons (I), ERα^{LH} neurons (L), and ERα^{POAH} neurons (O) at the baseline and after E_2 treatment (100 nM) in the presence or absence of IAA-94 (100 μM), with TTX (1 μM), CNQX (30 μM), D-AP5 (30 μM), and bicuculline (50 μM). Data are presented as means ± SEM with individual data points. $^{****}P < 0.0001$ in two-way ANOVA analysis followed by Šídák comparisons.

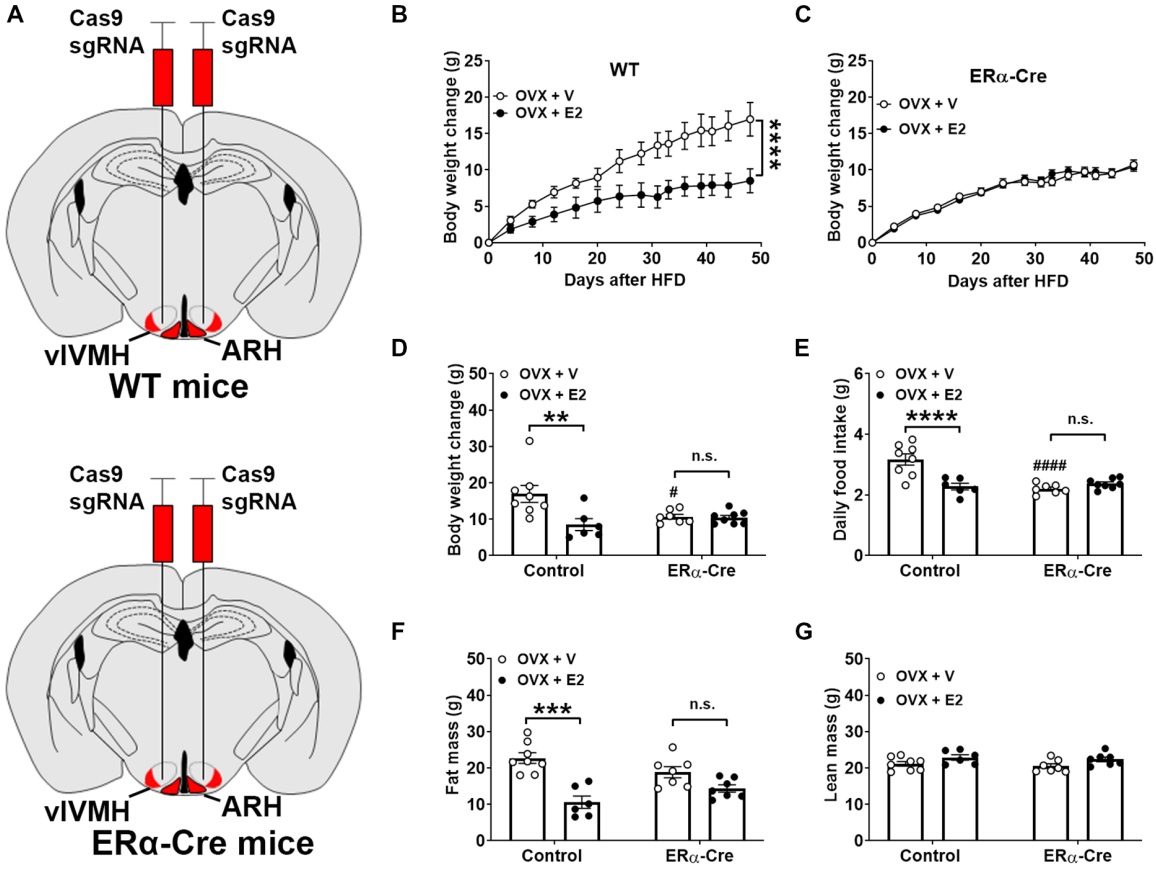

Fig. 5. Clic1 in ERα^{vlVMH} and ERα^{ARH} neurons mediates effects of E_2 fluctuations on energy balance in female mice. (**A**) A schematic illustration of Clic1 genetic disruption in ERα^{vlVMH} and ERα^{ARH} neurons in ERα-Cre mice and using WT littermates as controls. (**B** and **C**) Temporal changes in body weight in HFD-fed WT (B) and ERα-Cre (C) female mice in response to OVX + V versus OVX + E_2 treatment. Data are presented as means ± SEM. $N = 6$, 7, or 8 mice per group. ****$P < 0.0001$ in two-way ANOVA analysis. (**D**) Body weight changes on day 48 in mice described in (B and C). (**E**) Averaged daily food intake in mice described in (B and C). (**F** and **G**) Fat (F) and lean (G) mass of mice described in (B and C). Data are presented as means ± SEM. $N = 6$, 7, or 8 mice per group. **$P < 0.01$ or ***$P < 0.001$ between OVX + V and OVX + E_2 groups; #$P < 0.05$ or ####$P < 0.0001$ between WT and ERα-Cre mice in two-way ANOVA analysis followed by Šídák comparisons.

received OVX surgeries to deplete the ovarian hormones, and then they were further divided into two groups to receive either vehicle (OVX + V) or E_2 (OVX + E_2) treatment while being fed an obesogenic high-fat diet (HFD). Compared to OVX + V WT females, OVX + E_2 WT females showed significantly reduced body weight gain and fat mass, associated with reduced food intake, while lean mass remained comparable between the two groups (Fig. 5, B to G). OVX + E_2 treatment in ERα-Cre female mice did not induce any changes in body weight, fat/lean mass, and food intake compared to OVX + V ERα-Cre females (Fig. 5, B to G). It is also notable that the body weight gain and food intake in OVX + V ERα-Cre were significantly smaller than those in OVX + V WT females (Fig. 5, D and E). These results indicate that the loss of Clic1 in the mediobasal hypothalamus rendered female mice less susceptible to obesity development induced by OVX and at the same time blocked the anti-obesity effects of E_2 supplement. Last, we examined the metabolic phenotypes in a new cohort of gonad-intact chow-fed female mice with or without Clic1 deleted in the mediobasal hypothalamus. We found no difference in body weight, blood glucose, food intake, O_2 consumption activity, and brown fat gene expression between the two groups (fig. S5, B to G). Notably, Clic1 deletion resulted in a significant and modest increase in the average length of estrous cycles without significant changes in each stage (fig. S5, H and I). Considering the significant effects observed in HFD-fed females, the lack of metabolic phenotypes during chow feeding suggests an important role of Clic1 specifically in the context of excess nutrition.

DISCUSSION

In the current study, we demonstrated that a chloride channel protein, Clic1, can physically interact with ERα with a preference to the membrane-bound ERα. We further demonstrated that Clic1-mediated currents can be enhanced by E_2. Clic1 currents are required to mediate the E_2-induced rapid excitations in multiple brain ERα populations that we tested. Last, we show that genetic disruption of Clic1 in the mediobasal hypothalamus blunts the regulations of E_2 on female energy balance.

In addition to the well-known effects on gene transcription, E_2 can also trigger rapid signaling cascades in cells, including neurons (*46*). Some of these rapid actions of E_2 are mediated through the GPER (*27*). Other membrane receptors were also implicated as ERs (*47*, *48*), although the genes encoding these putative receptors have not been identified. Although ERα is traditionally known as a nuclear receptor, a subpopulation of ERα proteins also bind to the cell

membrane (*49*, *50*). Palmitoylation of ERα at the C451 residual is required for the receptor to localize to the plasma membrane, which further facilitates its association with caveolin-1 (*51*). Membrane-bound ERα mediates E_2-initiated rapid signaling, e.g., AMPK (*45*), cyclic adenosine 3′,5′-monophosphate (*52*) and phosphatidylinositol 3-kinase (*53*). The C451A mutation disrupts the ERα palmitoylation and therefore reduces its binding to the cell membrane and subsequently reduces these E_2-initiated rapid signaling (*34*, *35*). Notably, the C451A mutation has been reported to impair estrogenic actions on sexual behavior (*17*), fertility (*18*), energy, and glucose balance (*19*, *20*), indicating that signals initiated by membrane-bound ERα play indispensable roles in estrogen biology.

In addition to activating several rapid intracellular signals, E_2 or ERα agonists can also trigger excitation of a neuron within a timescale of milliseconds (*13*, *21*–*26*). These effects can be blocked by ERα deletion or by ERα-C451A mutation (*21*), indicating that actions of the membrane-bound ERα mediate this rapid electrophysiological event. Several ion channels have been implicated in E_2-initiated neuronal excitation. For example, E_2 can enhance L-type voltage-dependent calcium currents (L-VDCC) in hippocampal neurons, but these effects do not require ERs (*54*). In hypothalamic neurons, E_2 can reduce G protein–gated inwardly rectifying potassium (GIRK) currents triggered by other GPCRs, e.g., mu-opioid receptor and $GABA_B$ receptor (*55*). Effects of E_2 on GIRK currents are not affected by ERα or ERβ knockout (*47*), suggesting the involvement of other ERs. A putative membrane ER coupled to G_q (G_q-mER) has been proposed to mediate E_2 actions on GIRK (*47*), although the gene encoding this putative receptor has not been identified. Further, E_2 was also reported to regulate the small conductance calcium-activated potassium (SK) currents (*55*) and the adenosine 5′-triphosphate (ATP)–sensitive potassium (K_{ATP}) currents in hypothalamic neurons (*56*). Similarly, these effects of E_2 on SK and K_{ATP} currents are mediated via the putative G_q-mER (*57*), but not via ERα. Here, we reported that Clic1 forms the protein-protein complex with ERα. The Clic1-mediated chloride currents are regulated by E_2 signaling and are required to mediate E_2-induced excitation of ERα-expressing neurons. Consistently, a few early studies reported effects of E_2 on membrane chloride conductance in non-neuronal cells (*58*–*61*), although the molecular basis for these actions was never explored. Here, we provided both biochemical and biophysical evidence that membrane-bound ERα physically interacts with the Clic1 chloride channel, and activation of the receptor can trigger rapid neuronal excitation through Clic1 currents. We further speculate that the physical interactions between ERα and Clic1 proteins may provide a molecular basis for E_2 signals to cause rapid conformational changes in the Clic1 channel structure, resulting in altered ion conductance. Detailed structural analyses of the ERα-Clic1 complex would be warranted to further confirm this speculation. Notably, ERα is also reported to interact with VDAC1, which primarily locates at the outer mitochondrial membrane (*38*). The functional relevance of this ERα-VDAC1 remains unknown, and our results indicate that VDAC1 is not involved in E_2-induced excitation in $ERα^{vlVMH}$ neurons.

It is worth noting that while E_2 treatment can enhance the ERα-Clic1 interaction, there is a baseline interaction between the two proteins even in the absence of E_2 signals. Consistently, Clic1-mediated currents are detectable in $ERα^{vlVMH}$ neurons from OVX mice, although they are notably reduced compared to sham mice. Similarly, male $ERα^{vlVMH}$ neurons also exhibit smaller amount of Clic1 currents. These patterns suggest that Clic1 is involved in the constitutive actions of ERα independent of its ligand (*62*, *63*), a possibility that remains to be further examined. In addition, the membrane Clic1 channel likely is also under regulations by other hormonal and/or neural signals and therefore maintains certain baseline activity in the absence of E_2. In addition, we noted considerable interactions between the Clic1 protein and the ERα-C451A mutant protein, which does not bind to the cell membrane. Thus, the ERα-Clic1 protein complex also exists inside cells, which may also have biological functions. Other Clic family members have been implicated in mitochondrial membrane integrity (*64*) or inflammasome activation (*65*). The physiological relevance of the ERα-Clic1 complex inside cells warrants future investigations.

ERα-expressing neurons in both the mediobasal hypothalamus have been well established to be key neural populations that mediate anti-obesity effects of E_2 in females (*29*, *41*–*45*). In line with the demonstrated role of Clic1 in mediating E_2-induced excitation in $ERα^{vlVMH}$ and $ERα^{ARH}$ neurons, we found that loss of Clic1 in the mediobasal hypothalamus abolished the weight-lowering effects of E_2 supplement in HFD-fed OVX females. Notably, Clic1 expression may also be affected in the adjacent DMH, which could potentially contribute to the observed outcome, although there is no evidence for ERα in the DMH to regulate female body weight balance. Consistently, ERα-C451A mutant female mice with impaired membrane-bound ERα signaling exhibit increased susceptibility to HFD-induced obesity and metabolic disorders (*19*). Intriguingly, we also noted that OVX females with Clic1 disrupted in the mediobasal hypothalamus show reduced weight gain and food intake compared to OVX females with intact Clic1. In other words, the loss of Clic1 also renders female mice with reduced sensitivity to E_2 depletion. Consistent with this notion, a recent study reported that global Clic1 deficiency reduces weight gain in male mice (*66*), which to a certain degree resemble OVX females. These findings also suggest that Clic1 plays distinct roles in male versus female energy homeostasis, probably through its estrogen-dependent versus estrogen-independent actions. Similar to the opposite functions of Clic1 in male versus female animals, another molecule, interleukin-6 (IL-6), has been reported to promote male body weight gain but prevent female weight gain through its actions in the muscle (*67*, *68*). Alternatively, the lack of Clic1 may cause compensatory elevations in ERα signaling as a nuclear receptor that may contribute to the reduced weight gain induced by OVX. ERα as a nuclear receptor is known to enhance expression of leptin receptor and its downstream melanocortin receptors (*41*, *43*); OVX is associated with elevations in circulating leptin whose actions could be further amplified by increased ERα actions as a nuclear receptor. In addition, Clic1 may be also functionally involved in signaling of other ovarian hormones, e.g., progesterone. Notably, the progesterone receptor is another classic nuclear receptor with known rapid signaling (*28*), similar to ERα. All the speculations are worth further investigations to explore the functions of Clic1 in the context of female body weight regulation.

In addition to ERα, another ER classically known as a nuclear receptor, ERβ, has also been implicated in the regulation of body weight especially in the context of obegenic dietary challenge (*69*), although the exact ERβ-expressing neurons or cell types for these effects remain unclear. It is worth noting that a subpopulation of ERβ proteins can also bind to the cell membrane and trigger rapid signaling cascades (*51*) and rapidly regulate excitability of neurons (*9*, *28*). Thus, additional investigations are warranted to explore whether similar physical interactions between membrane ERβ and ion channel

proteins may exist as potential mechanisms for the rapid actions of ERβ on neuronal excitability. Notably, we showed that Clic1 partly mediates effects of AMPK on neuronal activity, implying that the AMPK pathway may be involved in the mechanism that regulates Clic1 functions, which warrants additional investigations.

In conclusion, we identified the Clic1 chloride channel as a key mediator for E_2/ERα-induced rapid neuronal excitation. This finding advances our understanding about the fundamental acting modes of the ovarian hormone. Clic1 is functionally involved in multiple ERα-expressing neurons in the brain. Given the diverse biological functions of E_2 via these neural populations, our findings may have a broad impact on multiple neurobiological processes, e.g., neuroendocrine, neurodevelopment, neurodegeneration, etc. These results revealed a new acting mode of ERs by physically interacting with membrane ion channels or other membrane proteins to mediate rapid actions of E_2. A conceivable limitation of our BioID approach is that we could only detect endogenous proteins in the tested cells; thus, the membrane proteins that interact with ERs in other cellular contexts are likely underestimated and deserve future investigations. Considering the emerging evidence for other nuclear receptors, e.g., progesterone receptor (*70*) and vitamin D receptor (*71*), to regulate neuronal excitability, we suggest that multiple hormone receptors, although classically known as nuclear receptors, can interact with membrane proteins to regulate cellular activities in a rapid manner.

MATERIALS AND METHODS

Study approval

Care of all animals and procedures were approved by the Institutional Animal Care and Use Committees at Baylor College of Medicine (AN-5479) or at Pennington Biomedical Research Center (IACUCPB-23-023).

Cell lines and vectors

HEK293T and Hela cells were cultured in Dulbecco's modified Eagle's medium (DMEM; Cytiva HyClone, SH3002201) supplemented with 10% (v/v) fetal bovine serum (FBS; Corning, 35016CV) at 37°C with 5% CO_2. To generate the N174-Flag-BioID construct, BioID (*31*) was incorporated into the lentiviral vector N174-MCS (Addgene, #81068) using the Gibson assembly strategy facilitated by a DNA assembly kit (NEB, E2621S). Subsequently, for the creation of the N174-Flag-BioID-ERα construct, the full-length human ERα was introduced into N174-Flag-BioID via Gibson assembly strategy. In the construction of the Flag-Clic1 construct, the full-length human Clic1 sequence was integrated into the retroviral backbone vector pCL-2xFlag. For the development of the ERα-EGFP construct, the full-length human ERα was initially cloned into the pENTR/D-TOPO vector using the TOPO cloning strategy. Subsequently, the full-length human ERα in the pENTR/D-TOPO vector was transferred to the destination vector pDEST-CMV-EGFP (Addgene, #122844) through the gateway cloning technology, resulting in the generation of the ERα-EGFP expression vector.

Generation of stable cell line

A stable cell line expressing BioID-ERα (or BioID only) was generated through lentivirus transduction by cotransfecting the lentiviral vector N174-BioID-ERα (or N174-BioID as a negative control) into HEK293T cells along with lentiviral packaging plasmids pMD2G and psPAX2 using Lipofectamine 3000 (Invitrogen, L3000015) following the manufacturer's recommendations. After 48 hours after transfection, the medium containing lentivirus was promptly collected for transduction. Hela cells were preseeded in a six-well plate before transduction. The culture medium containing lentivirus, supplemented with polybrene (8 μg/ml), was added to the Hela cells and incubated for 24 hours. Subsequently, the medium was replaced with fresh medium devoid of lentivirus for an additional day of culture. Puromycin was then used for the selection of transduced cells. Validation of BioID-ERα expression in the stable cell line was carried out through Western blotting.

BioID-mediated proximity labeling and MS analysis

The stable cells expressing BioID-ERα (with BioID only as a negative control) were cultured in 50 μM biotin (Sigma-Aldrich, B4639) for 16 hours. The cells were harvested, and the cytoplasmic, membrane, and nuclear fraction were separated by the subcellular protein fractionation kit (Thermo Fisher Scientific, #78840). Subsequently, the cytoplasmic and membrane protein extracts were used for BioID pull-down. There are four experimental groups including: (i) BioID Hela cells (cytoplasmic fraction), (ii) BioID Hela cells (membrane fraction), (iii) BioID-ERα Hela cells (cytoplasmic fraction), and (iv) BioID-ERα Hela cells (membrane fraction). In the pull-down experiment, the protein extracts were incubated with streptavidin magnetic beads (Thermo Fisher Scientific, 88816) to selectively retrieve biotinylated proteins. The collected beads, enriched with biotinylated proteins, were then subjected to liquid chromatography tandem mass spectrometry (MS) (Taplin Biological Mass Spectrometry Facility at Harvard Medical School) to elucidate the ERα proximity interaction network. For data analysis, a stringent criterion was applied to ensure the reliability of the results. Proteins in the BioID-ERα group exhibiting a sum intensity over 20 times that of the control group were specifically chosen as ERα-binding protein candidates. Subsequently, all identified protein candidates from BioID-MS underwent further analysis using the David Bioinformatics database (https://david.ncifcrf.gov/summary.jsp). This analysis aimed to categorize membrane proteins based on their cellular component annotations within the database.

Co-immunoprecipitation

HEK293T cells were transiently transfected with Flag-Clic1 and ERα-WT-EGFP (or ERα-C451A-EGFP) expression plasmids using Lipofectamine 3000 (Invitrogen, L3000015). To determine the effect of E_2 on the interaction between Clic1 and ERα, cells were treated with 10 nM β-estradiol for 30 min after 48 hours of transfection. Then, cells were harvested and lysed with NP-40 buffer and subjected to sonication at 20% amplitude for five cycles (5-s on and 20-s off). The resulting clear lysate was incubated with anti-Flag M2 beads (Sigma-Aldrich, M8823) at 4°C for 1 hour. Following incubation, the beads were washed three times with NP-40 buffer and three times with Tris buffered saline with Tween 20 (TBST) buffer. The precipitates were subsequently analyzed by immunoblotting using appropriate antibodies.

In-tube immunoprecipitation

In-tube immunoprecipitation was used to explore the interaction between Clic1 and ERα. Briefly, 3 nM human recombinant proteins Clic1 (Abcam, ab95486) and ERα (*72*) were incubated at 4°C for 1 hour in a test tube. Subsequently, the antibody against Clic1 (Cell Signaling Technology, 53424S) was introduced to precipitate the Clic1

protein complex. Meanwhile, normal rabbit immunoglobulin G was used as a negative control (Cell Signaling Technology, 2729). Following the antibody incubation, protein A beads (Cell Signaling Technology, 73778S) were added to capture the antigen-antibody complex. Six washes were performed using NP-40 buffer and TBST buffer. The protein complexes were eluted from the beads and subjected to further detailed analysis.

Western blotting

For immunoblot assay, the proteins from immunoprecipitation or other cell samples were electrophoresed on a 10% SDS–polyacrylamide gel and then subsequently transferred to polyvinylidene difluoride membrane. The membranes were probed with antibodies against ERα (Cell Signaling Technology, 8644S), GFP (Cell Signaling Technology, 2956S), Clic1 (Cell Signaling Technology, 53424S), and horseradish peroxidase–conjugated streptavidin (Boster, BA1088) at 4°C overnight. The membranes were then incubated with Alexa Fluor Plus 800–conjugated secondary antibody (A32735, Invitrogen) for 1 hour. Target bands were detected using a fluorescence scanner (Odyssey Infrared Imaging System, LI-COR Biotechnology). Bands were quantified using ImageJ software.

Mice

ERα-C451A heterozygous mice (*35*) were crossed with ERα-C451A heterozygous mice to generate ERα-C451A homozygous mice. The mouse ERα-ZsGreen transgene (*36*) was introduced to these crosses to label ERα neurons with ZsGreen. ERα-Cre mice were purchased from the Jackson Laboratory (#017911), which express Cre recombinase selectively in ERα-expressing neurons (*3*). Care of all animals and procedures were approved by the Institutional Animal Care and Use Committees at Baylor College of Medicine or at Pennington Biomedical Research Center. Mice were housed in a temperature-controlled environment in groups of two to four at 22° to 24°C using a 12-hour light and 12-hour dark cycle. The mice were fed with standard chow diet (5V5R, PicoLab) unless mentioned otherwise, and water was provided ad libitum.

Ovariectomy (OVX) and castration (CAST)

Female ERα-ZsGreen mice (12 weeks of age) were anesthetized with inhaled isoflurane. As previously described, bilateral OVX or sham surgeries were performed (*21*, *73*). For CAST surgery, 12-week-old male ERα-ZsGreen mice were anesthetized with inhaled isoflurane. As previously described, bilateral CAST or sham surgeries were performed in male mice (*73*). For sham surgeries, female or male ERα-ZsGreen mice (12 weeks of age) underwent the same anesthesia and surgical procedures (except for the removal of ovaries or testes). Four weeks after the surgery, sham, OVX, or CAST mice were used for electrophysiology or qPCR analysis.

Quantitative PCR

Mice were euthanized, and the mediobasal hypothalamus samples were collected. Total RNAs were extracted using the PicoPure RNA Isolation Kit (Thermo Fisher Scientific, #KIT0204) and then processed to cDNA for quantitative PCR (qPCR) test using qScript cDNA SuperMix (VWR, #101414-106). qPCR primers are as follows: Hprt (the housekeepinggene)(forward:5'-GTCAACGGGGGACATAAAAG-3′; reverse: 5'-CAACAATCAAGAC ATTCTTTCCA-3′ and Clic1 (forward: 5'-AAGAACAACCTCAGGTCGAAC-3′; reverse: 5'-CTCTGTCCGTCTCTTGGTGTC-3′.

CRISRP-Cas9 deletion of Clic1

The AAV vector carrying sgRNAs targeting mouse Clic1 was designed and constructed by Biocytogen (Wakefield, MA). The exon 2 and exon 5 were chosen to be targeted by CRISPR-Cas9. A total of 19 sgRNAs were designed with 7 targeting exon 4 and 12 targeting exon 11. These sgRNAs were selected using the CRISPR tool (www.sanger.ac.uk/htgt/wge/) with minimal potential off-target effects. All 14 sgRNAs (7 sgRNAs for each exon) were screened for on-target activity using a Universal CRISPR Activity Assay (Biocytogen) (*74*). Briefly, the plasmid carrying Cas9 and sgRNA and another plasmid carrying the target sequence cloned inside a luciferase gene were co-transfected into HEK293. Stop codon and CRISPR-Cas9 targeting sites were located within the luciferase gene. Stop codon induced the translational termination of the luciferase gene, while sgRNA targeting site cutting induced DNA annealing based on single-strand annealing and the complementary sequence recombination thereby occurred to rescue a complete coding sequence of the luciferase. The luciferase signal was then detected to reflect the DNA editing efficiency of the sgRNA. We used the pCS(puro)-positive plasmid, which expressed a proven positive sgRNA, as the positive control. The sgRNA#2 (GCAGTGATGGTGCCAAGATT GGG) and sgRNA#9 (TGAAACCAGCGCCGAAGATG AGG) were selected to target exon 2 and exon 5 of the Clic1 gene, respectively, due to their relatively high on-target activity and low off-target potentials. We then constructed an AAV-U6-sgRNA-tdTomato vector containing two sgRNAs (AAV-Clic1/sgRNAs-FLEX-tdTOMATO). Briefly, U6 promoter-sgRNAs, CAG promoter-flex-tdTomato-bGH polyA cassettes were cloned into the Addgene plasmid #61591 vector (www.addgene.org/61591/) and further verified by full sequencing. The virus was packaged by the Baylor IDDRC Neuroconnectivity Core.

To validate AAV-Clic1/sgRNAs-FLEX-tdTOMATO in mice, female ERα-Cre mice (12 weeks of age) received stereotaxic injections of AAV-FLEX-saCas9 [80 nl, 1×10^{13} genome copies (GC) per ml; Vector Biolabs, #7122] and AAV-Clic1/sgRNAs-FLEX-tdTOMATO (160 nl, 1.4×10^{12} GC per ml) into one side of the vlVMH (knockout side) and received AAV-Clic1/sgRNAs-FLEX-tdTOMATO (160 nl) and the AAV-FLEX-GFP (80 nl, 4.3×10^{13} GC per ml, no Cas9; Addgene, 100043-AAV9) in the other side of the vlVMH virus [control side; mediolateral (ML), ±0.75 mm; anteroposterior (AP), −1.60 mm; dorsoventral (DV), −5.85 mm]. After a 4-week recovery, these mice were subjected to single neuron genomic DNA analysis to detect if the CRISPR-Cas9 approach successfully induced the mutation of Clic1. Briefly, the two-step touchdown PCR was performed with each reaction containing 1 single $ERα^{vlVMH}$ neuron that was handpicked under the microscope. In the knockout side, $ERα^{vlVMH}$ neurons were labeled by tdTOMATO but not GFP, and in the control side, $ERα^{vlVMH}$ neurons were labeled by both tdTOMATO and GFP. The first primer pair across the sgRNA target region of Clic1, 5′- ATGCCCTCTTCTGGTGTGTC-3′ and 5′-GACAGCAACACTGGACTGGT-3′ [989 base pairs (bp)], were used for the first step of PCR. The PCR products were then used for the second step of PCR with the primer pair: 5'-TGGAGAACCATTGAGGAAGACAA-3' and 5'-AACCCCGTTTGTGTTTTGCC-3' (707 bp). To ensure the success of the neuron picking, two control primer pairs for an irrelevant gene (*Gabra5*) were also included to amplify the nonrelevant region of the genome. The first primer pair was 5′-CCTGTAAGAGTAGCCTGGCAT-3′ and 5′-AGATAAGAGACGTGGGGCTG-3′ (744 bp), and the second primer pair was 5′-AAGGAATCCAGTGACCAGCC-3′ and

5′-TCCTAAGGAACCAGCATGGG-3′ (525 bp) (*75*). Because a few samples from the knockout side still showed WT sequence of the Clic1, we suspected that these single neuron samples could have been contaminated by debris from the adjacent cells (that were not ERα-expressing neurons). Thus, we continued to validate the Clic1 disruption at the functional level using electrophysiology recordings for IAA-94–sensitive Clic1 currents, as described below.

Electrophysiology

All electrophysiological experiments were performed in female mice (>10 weeks of age) at diestrus. Mice were deeply anesthetized with isoflurane and transcardially perfused with a modified ice-cold sucrose-based cutting solution (pH 7.3) containing 10 mM NaCl, 25 mM $NaHCO_3$, 195 mM sucrose, 5 mM glucose, 2.5 mM KCl, 1.25 mM NaH_2PO_4, 2 mM Na-pyruvate, 0.5 Mm $CaCl_2$, and 7 mM $MgCl_2$, bubbled continuously with 95% O_2 and 5% CO_2 (*76*, *77*). The mice were then decapitated, and the entire brain was removed and immediately submerged in the cutting solution. Slices (250 μm) were cut with a Leica VT1000 S vibrating microtome (Leica Biosystems, IL). Three to four brain slices containing the vlVMH, ARH, LH, MeA, BNST, and POAH were obtained for each animal. The slices were recovered for 1 hour at 34°C and then maintained at room temperature in artificial cerebrospinal fluid (aCSF; pH 7.3) containing 126 mM NaCl, 2.5 mM KCl, 2.4 mM $CaCl_2$, 1.2 mM NaH_2PO_4, 1.2 mM $MgCl_2$, 5.0 mM glucose, and 21.4 mM $NaHCO_3$ saturated with 95% O_2 and 5% CO_2 before recording (*76*, *77*).

Slices were transferred to a recording chamber and allowed to equilibrate for at least 10 min before recording. The slices were superfused at 34°C in oxygenated aCSF at a flow rate of 1.8 to 2 ml/min. Patch pipettes with resistances of 3 to 5 megohm were filled with intracellular solution (pH 7.3) containing 128 mM K-gluconate, 10 mM KCl, 10 mM Hepes, 0.1 mM EGTA, 2 mM $MgCl_2$, 0.05 mM Na–guanosine 5′-triphosphate, and 0.05 mM Mg-ATP. Recordings were made using a MultiClamp 700B amplifier (Axon Instrument), sampled using Digidata 1440 A, and analyzed offline with pClamp 10.3 software (Axon Instruments). Series resistance was monitored during the recording, and the values were generally <10 megohm and were not compensated. The liquid junction potential was +12.5 mV and was corrected after the experiment. Data were excluded if the series resistance increased notably during the experiment or without overshoot for action potential. Currents were amplified, filtered at 1 kHz, and digitized at 10 kHz.

To measure IAA-94–sensitive Clic1 currents, the bath solution contains 130 mM NaCl, 5.5 mM KCl, 24 mM Hepes, 1 mM $MgCl_2$, 0.5 mM $CaCl_2$, and 5 mM D-glucose (pH 7.4); the pipette solution contains 128 mM *N*-methyl-glucamine-Cl, 5 mM KCl, 2.5 mM $CaCl_2$, 1 mM $MgCl_2$, 10 mM Hepes, 5 mM glucose, 10 mM tetraethylammonium-Cl, and 0.03 mM margatoxin (pH 7.3 to 7.4) with chloride acid (*58*). Total Clic1 current was recorded under the voltage-clamp mode by holding the membrane potential at −60 mV in the presence of 1 μM TTX (a reversible, selective, and high-affinity inhibitor of voltage-gated sodium channels), 10 μM TTA-P2 (a T-type calcium channel blocker), 50 μM nifedipine (an L-type calcium channel blocker), and 5 mM 4-aminopyridine (a potassium-selective ion channel blocker) (*78*). At intervals, neurons were voltage clamped from −80 to +80 mV in a ramp protocol for 1 s (*58*). Then, the neurons were perfused with 100 μM indanyloxyacetic acid 94 (a chloride channel inhibitor; Sigma-Aldrich, #I117) (*37*, *79*) and/or 100 μM IAA-94 mixed with 100 nM E_2 with for 3 min. The Clic1 current was calculated by subtracting the left current in the presence of IAA-94 from total current without IAA-94. In another experiment, IAA-94–sensitive current was also recorded with chloride-free pipette solution contains 92 mM NMDG, 1.25 mM NaH_2PO_4, 30 mM $NaHCO_3$, 20 mM Hepes, 5 mM glucose, 3 mM Na-pyruvate, and 10 mM $MgSO_4{\cdot}7H_2O$ (pH to 7.3 to 7.4) with phosphoric acid.

The current clamp was engaged to test neural firing frequency and resting membrane potential after vehicle or E_2 (10, 100, or 1000 nM) puff treatment (5 s). The values for resting membrane potential and firing frequency averaged within 2-min bin after vehicle or E_2 treatment (*80*). If the resting membrane potential of a neuron depolarized more than 2 mV (≥2 mV) in amplitude, then we defined it as activation. After the identification of an E_2-activated neuron, the same neuron will be puff treated with 100 nM E_2 in the presence of 100 μM IAA-94. To measure the membrane input resistance in $ERα^{vlVMH}$ neurons, all neurons were held at −60 mV with holding current. The hyperpolarizing current pulses ranging from −160 to 0 mV with 20 mV increase in each step (1-s duration) were applied on the $ERα^{vlVMH}$ neurons. The input resistance was calculated by using the slope of the linear fit between the voltage responses and current injections. To test the effect of the AMPK activator on $ERα^{vlVMH}$ neurons, neurons were puff treated by 10 μM A769662 in the presence of vehicle or IAA-94 (*81*). To test if other ERs are regulated by E_2 in $ERα^{vlVMH}$ neurons, $ERα^{vlVMH}$ neurons were pretreated with 10 μM G15 (a high-affinity and selective GPER receptor antagonist) (*82*) or 50 μM PHTBB (a selective estrogen ERβ receptor antagonist) before the E_2 treatment (*83*). To test if E_2 regulates VDAC1 ion channel, $ERα^{vlVMH}$ neurons was pretreated with 20 μM VBIT-12 (a potent inhibitor of VDAC1) before the E_2 treatment (*39*, *84*).

To exclude the possible circuitry inputs to the recorded neurons, the neurons were pre-incubated with a cocktail blockers containing 1 μM TTX, 30 μM CNQX (a potent non-NMDA glutamate receptor antagonist), 30 μM D-AP5 (a potent and selective NMDA receptor antagonist), and 50 μM bicuculline (a $GABA_A$ receptor antagonist) to block the excitatory and inhibitory input in the recorded ERα neurons (*80*, *85*). Resting membrane potential was calculated after E_2 treatment with vehicle or 100 μM IAA-94.

Deletion of Clic1 from $ERα^{vlVMH}$ and $ERα^{AR}$ neurons

ERα-Cre female mice and their WT control littermates (10 weeks) were anesthetized by isoflurane and received bilateral stereotaxic injections of AAV-Clic1/sgRNAs-FLEX-tdTOMATO and AAV-FLEX-saCas9Biolabs) into the mediobasal hypothalamus that contains both the vlVMH and ARH (ML, ±0.5 mm; AP, −1.55 mm; DV, −5.85 mm). During the same surgery, the bilateral ovariectomy (OVX) were performed in these female mice as previously described (*41*, *86*, *87*). These mice were singly housed and allowed to recover from the surgery for 1 month. Then, they were fed with an HFD (60% fat; D12492i, Research Diets) and received subcutaneous injections of vehicle (50 μl of sesame oil; Sigma-Aldrich, S3547) or E_2 (2 μg in 50 μl of sesame oil; Sigma-Aldrich, E8875) every 4 days until the end of study. Body weight and food intake were measured every 4 days. Quantitative magnetic resonance was used to determine body composition at the end of the study. At the end of the study, all mice were anesthetized with inhaled isoflurane and quickly perfused with saline, followed by 10% formalin. After dehydration with 30% sucrose, brains were processed for frozen sectioning at 25 μm, and these brain sections were subjected to post hoc histo were included in the data analyses.

Another cohort of female ERα-Cre and their WT control littermates (10 weeks) were used to generate mice lacking Clic1 in ERα neurons in the mediobasal hypothalamus and controls, as described above. These mice were singly housed and fed on regular chow diet (5V5R, PicoLab). Body weight and food intake were monitored every 4 days. Blood glucose was measured at day 8, day 16, and day 24 after surgery. The estrous cycle was monitored via virginal smears at day 7 after surgery for 23 days continuously. On day 48 after surgery, mice were put into TSE PhenoMaster metabolic cages to measure O_2 consumption. At the end of the study, all mice were anesthetized with inhaled isoflurane, and blood was collected and processed to serum samples, which were subjected to the measurement of follicle-stimulating hormone and luteinizing hormone using ELISA kits (Abclonal, #RK04237 and #RK15292). Uterus and ovaries were collected and weighed. Brown adipocyte tissue was collected and subjected to qPCR, similarly as described above. PCR primers: actin (forward, 5′-ATGGAGGGGAATACAGCCC-3′; reverse, 5′-TTCTTTGCAGCTCCTTCGTT-3′), Ucp1 (forward, 5′-CACGGGGACCTACAATGCTT-3′; reverse, 5′-TAGGGGTCGTCCCTTTCCAA-3′), Esr1 (forward, 5′-GAACGAGCCCAGCGCCTACG-3′; reverse, 5’-TCTCGGCCATTCTGGCGTCG-3′), Pgc1a (forward, 5′-TGATGTGAATGACTTGGATACAGACA-3′; reverse, 5′-GCTCATTGTTGTACTGGTTGGATATG-3′), Cidea (forward, 5′-ATCACAACTGGCCTGGTTACG-3′; reverse, 5′-TACTACCCGGTGTCCATTTCT-3′), Dio2 (forward, 5′-AATTATGCCTCGGAGAAGACCG-3′; reverse, 5′-GGCAGTTGCCTAGTGAAAGGT-3′), and Prdm16 (forward, 5′-TGACGGATACAGAGGTGTCAT-3′; reverse, 5′-ACGCTAC-ACGGATGTACTTGA-3′).

Statistical analyses

The data are presented as means ± SEM or as individual data points. Statistical analyses were performed using GraphPad Prism 7.0 to evaluate normal distribution and variations within and among groups. Methods of statistical analyses were chosen on the basis of the design of each experiment and are indicated in figure legends or main text. $P < 0.05$ was considered to be statistically significant.

Supplementary Materials

The PDF file includes:
Figs. S1 to S5
Legend for table S1

Other Supplementary Material for this manuscript includes the following:
Table S1

REFERENCES AND NOTES

1. S. L. Dubois, M. Acosta-Martinez, M. R. DeJoseph, A. Wolfe, S. Radovick, U. Boehm, J. H. Urban, J. E. Levine, Positive, but not negative feedback actions of estradiol in adult female mice require estrogen receptor α in kisspeptin neurons. *Endocrinology* **156**, 1111–1120 (2015).
2. T. M. Wintermantel, R. E. Campbell, R. Porteous, D. Bock, H. J. Grone, M. G. Todman, K. S. Korach, E. Greiner, C. A. Perez, G. Schutz, A. E. Herbison, Definition of estrogen receptor pathway critical for estrogen positive feedback to gonadotropin-releasing hormone neurons and fertility. *Neuron* **52**, 271–280 (2006).
3. H. Lee, D. W. Kim, R. Remedios, T. E. Anthony, A. Chang, L. Madisen, H. Zeng, D. J. Anderson, Scalable control of mounting and attack by Esr1$^+$ neurons in the ventromedial hypothalamus. *Nature* **509**, 627–632 (2014).
4. P. Pavlidi, N. Kokras, C. Dalla, Antidepressants' effects on testosterone and estrogens: What do we know? *Eur. J. Pharmacol.* **899**, 173998 (2021).
5. R. Santos-Toscano, M. A. Arevalo, L. M. Garcia-Segura, D. Grassi, N. Lagunas, Interaction of gonadal hormones, dopaminergic system, and epigenetic regulation in the generation of sex differences in substance use disorders: A systematic review. *Front. Neuroendocrinol.* **71**, 101085 (2023).
6. R. J. Handa, M. J. Weiser, Gonadal steroid hormones and the hypothalamo-pituitary-adrenal axis. *Front. Neuroendocrinol.* **35**, 197–220 (2014).
7. Y. Hara, E. M. Waters, B. S. McEwen, J. H. Morrison, Estrogen effects on cognitive and synaptic health over the lifecourse. *Physiol. Rev.* **95**, 785–807 (2015).
8. E. J. Spary, A. Maqbool, T. F. Batten, Oestrogen receptors in the central nervous system and evidence for their role in the control of cardiovascular function. *J. Chem. Neuroanat.* **38**, 185–196 (2009).
9. K. Saito, X. Cao, Y. He, Y. Xu, Progress in the molecular understanding of central regulation of body weight by estrogens. *Obesity* **23**, 919–926 (2015).
10. A. Frank, L. M. Brown, D. J. Clegg, The role of hypothalamic estrogen receptors in metabolic regulation. *Front. Neuroendocrinol.* **35**, 550–557 (2014).
11. M. H. Faulds, C. Zhao, K. Dahlman-Wright, J. A. Gustafsson, The diversity of sex steroid action: Regulation of metabolism by estrogen signaling. *J. Endocrinol.* **212**, 3–12 (2012).
12. Y. Xu, P. Huangyang, Y. Wang, L. Xue, E. Devericks, H. G. Nguyen, X. Yu, J. A. Oses-Prieto, A. L. Burlingame, S. Miglani, H. Goodarzi, D. Ruggero, ERα is an RNA-binding protein sustaining tumor cell survival and drug resistance. *Cell* **184**, 5215–5229.e17 (2021).
13. T. A. Roepke, J. Qiu, M. A. Bosch, O. K. Ronnekleiv, M. J. Kelly, Cross-talk between membrane-initiated and nuclear-initiated oestrogen signalling in the hypothalamus. *J. Neuroendocrinol.* **21**, 263–270 (2009).
14. A. Pedram, M. Razandi, J. K. Kim, F. O'Mahony, E. Y. Lee, U. Luderer, E. R. Levin, Developmental phenotype of a membrane only estrogen receptor α (MOER) mouse. *J. Biol. Chem.* **284**, P3488–P3495 (2009).
15. J. F. Arnal, F. Lenfant, R. Metivier, G. Flouriot, D. Henrion, M. Adlanmerini, C. Fontaine, P. Gourdy, P. Chambon, B. Katzenellenbogen, J. Katzenellenbogen, Membrane and nuclear estrogen receptor alpha actions: From tissue specificity to medical implications. *Physiol. Rev.* **97**, 1045–1087 (2017).
16. E. R. Levin, S. R. Hammes, Nuclear receptors outside the nucleus: Extranuclear signalling by steroid receptors. *Nat. Rev. Mol. Cell Biol.* **17**, 783–797 (2016).
17. C. de Bournonville, P. Lemoine, J. M. Foidart, J. F. Arnal, F. Lenfant, C. A. Cornil, Role of membrane estrogen receptor alpha (ERα) in the rapid regulation of male sexual behavior. *J. Neuroendocrinol.* **35**, e13341 (2023).
18. M. Rusidze, M. C. Faure, P. Sicard, I. Raymond-Letron, F. Giton, E. Vessieres, V. Prevot, D. Henrion, J. F. Arnal, C. A. Cornil, F. Lenfant, Loss of function of the maternal membrane oestrogen receptor ERα alters expansion of trophoblast cells and impacts mouse fertility. *Development* **149**, dev200683 (2022).
19. A. Fabre, B. Tramunt, A. Montagner, C. Mouly, E. Riant, M. L. Calmy, M. Adlanmerini, C. Fontaine, R. Burcelin, F. Lenfant, J. F. Arnal, P. Gourdy, Membrane estrogen receptor-α contributes to female protection against high-fat diet-induced metabolic disorders. *Front. Endocrinol.* **14**, 1215947 (2023).
20. C. Allard, J. J. Morford, B. Xu, B. Salwen, W. Xu, L. Desmoulins, A. Zsombok, J. K. Kim, E. R. Levin, F. Mauvais-Jarvis, Loss of nuclear and membrane estrogen receptor-α differentially impairs insulin secretion and action in male and female mice. *Diabetes* **68**, 490–501 (2019).
21. K. Yu, Y. He, I. Hyseni, Z. Pei, Y. Yang, P. Xu, X. Cai, H. Liu, N. Qu, M. Yu, C. Liang, T. Yang, J. Wang, P. Gourdy, J. F. Arnal, F. Lenfant, Y. Xu, C. Wang, 17β-estradiol promotes acute refeeding in hungry mice via membrane-initiated ERα signaling. *Mol. Metab.* **42**, 101053 (2020).
22. X. Cao, P. Xu, M. G. Oyola, Y. Xia, X. Yan, K. Saito, F. Zou, C. Wang, Y. Yang, A. Hinton Jr., C. Yan, H. Ding, L. Zhu, L. Yu, B. Yang, Y. Feng, D. J. Clegg, S. Khan, R. DiMarchi, S. K. Mani, Q. Tong, Y. Xu, Estrogens stimulate serotonin neurons to inhibit binge-like eating in mice. *J. Clin. Invest.* **124**, 4351–4362 (2014).
23. P. Xu, X. Cao, Y. He, L. Zhu, Y. Yang, K. Saito, C. Wang, X. Yan, A. O. Hinton Jr., F. Zou, H. Ding, Y. Xia, C. Yan, G. Shu, S. P. Wu, B. Yang, Y. Feng, D. J. Clegg, R. DeMarchi, S. A. Khan, S. Y. Tsai, F. J. DeMayo, Q. Wu, Q. Tong, Y. Xu, Estrogen receptor-α in medial amygdala neurons regulates body weight. *J. Clin. Invest.* **125**, 2861–2876 (2015).
24. K. Saito, Y. He, Y. Yang, L. Zhu, C. Wang, P. Xu, A. O. Hinton, X. Yan, J. Zhao, M. Fukuda, Q. Tong, D. J. Clegg, Y. Xu, PI3K in the ventromedial hypothalamic nucleus mediates estrogenic actions on energy expenditure in female mice. *Sci. Rep.* **6**, 23459 (2016).
25. J. Qiu, O. K. Ronnekleiv, M. J. Kelly, Modulation of hypothalamic neuronal activity through a novel G-protein-coupled estrogen membrane receptor. *Steroids* **73**, 985–991 (2008).
26. A. Malyala, C. Zhang, D. N. Bryant, M. J. Kelly, O. K. Ronnekleiv, PI3K signaling effects in hypothalamic neurons mediated by estrogen. *J. Comp. Neurol.* **506**, 895–911 (2008).
27. P. Thomas, Y. Pang, E. J. Filardo, J. Dong, Identity of an estrogen membrane receptor coupled to a G protein in human breast cancer cells. *Endocrinology* **146**, 624–632 (2005).
28. M. Zhang, H. Weiland, M. Schofbanker, W. Zhang, Estrogen receptors alpha and beta mediate synaptic transmission in the PFC and hippocampus of mice. *Int. J. Mol. Sci.* **22**, 1485 (2021).
29. L. Zhu, P. Xu, X. Cao, Y. Yang, A. O. Hinton Jr., Y. Xia, K. Saito, X. Yan, F. Zou, H. Ding, C. Wang, C. Yan, P. Saha, S. A. Khan, J. Zhao, M. Fukuda, Q. Tong, D. J. Clegg, L. Chan, Y. Xu, The ERα-PI3K cascade in pro-opiomelanocortin progenitor neurons regulates feeding and glucose balance in female mice. *Endocrinology* **156**, 4474–4491 (2015).

30. F. Cianci, I. Verduci, Transmembrane chloride intracellular channel 1 (tmCLIC1) as a potential biomarker for personalized medicine. *J. Pers. Med.* **11**, 635 (2021).
31. D. I. Kim, S. C. Jensen, K. A. Noble, B. Kc, K. H. Roux, K. Motamedchaboki, K. J. Roux, An improved smaller biotin ligase for BioID proximity labeling. *Mol. Biol. Cell* **27**, 1188–1196 (2016).
32. S. Averaimo, R. H. Milton, M. R. Duchen, M. Mazzanti, Chloride intracellular channel 1 (CLIC1): Sensor and effector during oxidative stress. *FEBS Lett.* **584**, 2076–2084 (2010).
33. S. Gururaja Rao, N. J. Patel, H. Singh, Intracellular chloride channels: Novel biomarkers in diseases. *Front. Physiol.* **11**, 96 (2020).
34. A. Pedram, M. Razandi, M. Lewis, S. Hammes, E. R. Levin, Membrane-localized estrogen receptor α is required for normal organ development and function. *Dev. Cell* **29**, 482–490 (2014).
35. M. Adlanmerini, R. Solinhac, A. Abot, A. Fabre, I. Raymond-Letron, A. L. Guihot, F. Boudou, L. Sautier, E. Vessieres, S. H. Kim, P. Liere, C. Fontaine, A. Krust, P. Chambon, J. A. Katzenellenbogen, P. Gourdy, P. W. Shaul, D. Henrion, J. F. Arnal, F. Lenfant, Mutation of the palmitoylation site of estrogen receptor α in vivo reveals tissue-specific roles for membrane versus nuclear actions. *Proc. Natl. Acad. Sci. U.S.A.* **111**, E283–E290 (2014).
36. K. Saito, Y. He, X. Yan, Y. Yang, C. Wang, P. Xu, A. O. Hinton Jr., G. Shu, L. Yu, Q. Tong, Y. Xu, Visualizing estrogen receptor-α-expressing neurons using a new ERα-ZsGreen reporter mouse line. *Metabolism* **65**, 522–532 (2016).
37. R. H. Milton, R. Abeti, S. Averaimo, S. DeBiasi, L. Vitellaro, L. Jiang, P. M. Curmi, S. N. Breit, M. R. Duchen, M. Mazzanti, CLIC1 function is required for β-amyloid-induced generation of reactive oxygen species by microglia. *J. Neurosci.* **28**, 11488–11499 (2008).
38. C. M. Ramirez, M. Gonzalez, M. Diaz, R. Alonso, I. Ferrer, G. Santpere, B. Puig, G. Meyer, R. Marin, VDAC and ERα interaction in caveolae from human cortex is altered in Alzheimer's disease. *Mol. Cell. Neurosci.* **42**, 172–183 (2009).
39. T. Xia, J. Yu, Y. Chen, X. Chang, M. Meng, Phosphoglycerate mutase 5 aggravates alcoholic liver disease through disrupting VDAC-1-dependent mitochondrial integrity. *Int. J. Med. Sci.* **21**, 755–764 (2024).
40. F. A. Duca, C. D. Cote, B. A. Rasmussen, M. Zadeh-Tahmasebi, G. A. Rutter, B. M. Filippi, T. K. Lam, Metformin activates a duodenal Ampk–dependent pathway to lower hepatic glucose production in rats. *Nat. Med.* **21**, 506–511 (2015).
41. Y. Xu, T. P. Nedungadi, L. Zhu, N. Sobhani, B. G. Irani, K. E. Davis, X. Zhang, F. Zou, L. M. Gent, L. D. Hahner, S. A. Khan, C. F. Elias, J. K. Elmquist, D. J. Clegg, Distinct hypothalamic neurons mediate estrogenic effects on energy homeostasis and reproduction. *Cell Metab.* **14**, 453–465 (2011).
42. S. M. Correa, D. W. Newstrom, J. P. Warne, P. Flandin, C. C. Cheung, A. T. Lin-Moore, A. A. Pierce, A. W. Xu, J. L. Rubenstein, H. A. Ingraham, An estrogen-responsive module in the ventromedial hypothalamus selectively drives sex-specific activity in females. *Cell Rep.* **10**, 62–74 (2015).
43. W. C. Krause, R. Rodriguez, B. Gegenhuber, N. Matharu, A. N. Rodriguez, A. M. Padilla-Roger, K. Toma, C. B. Herber, S. M. Correa, X. Duan, N. Ahituv, J. Tollkuhn, H. A. Ingraham, Oestrogen engages brain MC4R signalling to drive physical activity in female mice. *Nature* **599**, 131–135 (2021).
44. Q. Gao, G. Mezei, Y. Nie, Y. Rao, C. S. Choi, I. Bechmann, C. Leranth, D. Toran-Allerand, C. A. Priest, J. L. Roberts, X. B. Gao, C. Mobbs, G. I. Shulman, S. Diano, T. L. Horvath, Anorectic estrogen mimics leptin's effect on the rewiring of melanocortin cells and Stat3 signaling in obese animals. *Nat. Med.* **13**, 89–94 (2007).
45. P. B. Martinez de Morentin, I. Gonzalez-Garcia, L. Martins, R. Lage, D. Fernandez-Mallo, N. Martinez-Sanchez, F. Ruiz-Pino, J. Liu, D. A. Morgan, L. Pinilla, R. Gallego, A. K. Saha, A. Kalsbeek, E. Fliers, P. H. Bisschop, C. Dieguez, R. Nogueiras, K. Rahmouni, M. Tena-Sempere, M. Lopez, Estradiol regulates brown adipose tissue thermogenesis via hypothalamic AMPK. *Cell Metab.* **20**, 41–53 (2014).
46. F. Mauvais-Jarvis, C. A. Lange, E. R. Levin, Membrane-initiated estrogen, androgen, and progesterone receptor signaling in health and disease. *Endocr. Rev.* **43**, 720–742 (2022).
47. J. Qiu, M. A. Bosch, S. C. Tobias, A. Krust, S. M. Graham, S. J. Murphy, K. S. Korach, P. Chambon, T. S. Scanlan, O. K. Ronnekleiv, M. J. Kelly, A G-protein-coupled estrogen receptor is involved in hypothalamic control of energy homeostasis. *J. Neurosci.* **26**, 5649–5655 (2006).
48. C. D. Toran-Allerand, X. Guan, N. J. MacLusky, T. L. Horvath, S. Diano, M. Singh, E. S. Connolly Jr., I. S. Nethrapalli, A. A. Tinnikov, ER-X: A novel, plasma membrane-associated, putative estrogen receptor that is regulated during development and after ischemic brain injury. *J. Neurosci.* **22**, 8391–8401 (2002).
49. M. Razandi, A. Pedram, G. L. Greene, E. R. Levin, Cell membrane and nuclear estrogen receptors (ERs) originate from a single transcript: Studies of ERα and ERβ expressed in Chinese hamster ovary cells. *Mol. Endocrinol.* **13**, 307–319 (1999).
50. A. Pedram, M. Razandi, E. R. Levin, Nature of functional estrogen receptors at the plasma membrane. *Mol. Endocrinol.* **20**, 1996–2009 (2006).
51. A. Pedram, M. Razandi, R. C. Sainson, J. K. Kim, C. C. Hughes, E. R. Levin, A conserved mechanism for steroid receptor translocation to the plasma membrane. *J. Biol. Chem.* **282**, 22278–22288 (2007).
52. R. J. Pietras, C. M. Szego, Specific binding sites for oestrogen at the outer surfaces of isolated endometrial cells. *Nature* **265**, 69–72 (1977).
53. T. Simoncini, A. Hafezi-Moghadam, D. P. Brazil, K. Ley, W. W. Chin, J. K. Liao, Interaction of oestrogen receptor with the regulatory subunit of phosphatidylinositol-3-OH kinase. *Nature* **407**, 538–541 (2000).
54. S. N. Sarkar, R. Q. Huang, S. M. Logan, K. D. Yi, G. H. Dillon, J. W. Simpkins, Estrogens directly potentiate neuronal L-type $Ca2^+$ channels. *Proc. Natl. Acad. Sci. U.S.A.* **105**, 15148–15153 (2008).
55. M. J. Kelly, O. K. Ronnekleiv, N. Ibrahim, A. H. Lagrange, E. J. Wagner, Estrogen modulation of K^+ channel activity in hypothalamic neurons involved in the control of the reproductive axis. *Steroids* **67**, 447–456 (2002).
56. O. K. Ronnekleiv, M. A. Bosch, C. Zhang, Regulation of endogenous conductances in GnRH neurons by estrogens. *Brain Res.* **1364**, 25–34 (2010).
57. P. E. Micevych, M. J. Kelly, Membrane estrogen receptor regulation of hypothalamic function. *Neuroendocrinology* **96**, 103–110 (2012).
58. S. P. Hardy, M. A. Valverde, Novel plasma membrane action of estrogen and antiestrogens revealed by their regulation of a large conductance chloride channel. *FASEB J.* **8**, 760–765 (1994).
59. M. A. Valverde, S. P. Hardy, M. Diaz, Activation of Maxi Cl^- channels by antiestrogens and phenothiazines in NIH3T3 fibroblasts. *Steroids* **67**, 439–445 (2002).
60. Z. Li, Y. Niwa, S. Sakamoto, X. Chen, Y. Nakaya, Estrogen modulates a large conductance chloride channel in cultured porcine aortic endothelial cells. *J. Cardiovasc. Pharmacol.* **35**, 506–510 (2000).
61. M. Henriquez, G. Riquelme, 17β-estradiol and tamoxifen regulate a maxi-chloride channel from human placenta. *J. Membr. Biol.* **191**, 59–68 (2003).
62. J. T. Bridgham, J. Keay, E. A. Ortlund, J. W. Thornton, Vestigialization of an allosteric switch: Genetic and structural mechanisms for the evolution of constitutive activity in a steroid hormone receptor. *PLOS Genet.* **10**, e1004058 (2014).
63. J. Favre, E. Vessieres, A. L. Guihot, C. Proux, L. Grimaud, J. Rivron, M. C. Garcia, L. Rethore, R. Zahreddine, M. Davezac, C. Febrissy, M. Adlanmerini, L. Loufrani, V. Procaccio, J. M. Foidart, G. Flouriot, F. Lenfant, C. Fontaine, J. F. Arnal, D. Henrion, Membrane estrogen receptor alpha (ERα) participates in flow-mediated dilation in a ligand-independent manner. *eLife* **10**, e68695 (2021).
64. U. De Marchi, I. Szabo, G. M. Cereghetti, P. Hoxha, W. J. Craigen, M. Zoratti, A maxi-chloride channel in the inner membrane of mammalian mitochondria. *Biochim. Biophys. Acta* **1777**, 1438–1448 (2008).
65. T. Tang, X. Lang, C. Xu, X. Wang, T. Gong, Y. Yang, J. Cui, L. Bai, J. Wang, W. Jiang, R. Zhou, CLICs-dependent chloride efflux is an essential and proximal upstream event for NLRP3 inflammasome activation. *Nat. Commun.* **8**, 202 (2017).
66. R. C. Zapata, D. Zhang, D. Yoon, C. A. Nasamran, D. R. Chilin-Fuentes, A. Libster, B. S. Chaudry, M. Lopez-Valencia, D. Ponnalagu, H. Singh, M. Petrascheck, O. Osborn, Targeting Clic1 for the treatment of obesity: A novel therapeutic strategy to reduce food intake and body weight. *Mol. Metab.* **76**, 101794 (2023).
67. B. Ferrer, B. Navia, M. Giralt, G. Comes, J. Carrasco, A. Molinero, A. Quintana, R. M. Senaris, J. Hidalgo, Muscle-specific interleukin-6 deletion influences body weight and body fat in a sex-dependent manner. *Brain Behav. Immun.* **40**, 121–130 (2014).
68. A. Molinero, A. Fernandez-Perez, A. Mogas, M. Giralt, G. Comes, O. Fernandez-Gayol, M. Vallejo, J. Hidalgo, Role of muscle IL-6 in gender-specific metabolism in mice. *PLOS ONE* **12**, e0173675 (2017).
69. A. Foryst-Ludwig, M. Clemenz, S. Hohmann, M. Hartge, C. Sprang, N. Frost, M. Krikov, S. Bhanot, R. Barros, A. Morani, J. A. Gustafsson, T. Unger, U. Kintscher, Metabolic actions of estrogen receptor β (ERβ) are mediated by a negative cross-talk with PPARγ. *PLOS Genet.* **4**, e1000108 (2008).
70. S. Shiono, H. Sun, T. Batabyal, A. Labuz, J. Williamson, J. Kapur, S. Joshi, Limbic progesterone receptor activity enhances neuronal excitability and seizures. *Epilepsia* **62**, 1946–1959 (2021).
71. H. Liu, Y. He, J. Beck, S. da Silva Teixeira, K. Harrison, Y. Xu, S. Sisley, Defining vitamin D receptor expression in the brain using a novel VDR^{Cre} mouse. *J. Comp. Neurol.* **529**, 2362–2375 (2021).
72. P. Yi, Z. Wang, Q. Feng, G. D. Pintilie, C. E. Foulds, R. B. Lanz, S. J. Ludtke, M. F. Schmid, W. Chiu, B. W. O'Malley, Structure of a biologically active estrogen receptor-coactivator complex on DNA. *Mol. Cell* **57**, 1047–1058 (2015).
73. M. Luengo-Mateos, A. Gonzalez-Vila, A. M. Torres Caldas, A. M. Alasaoufi, M. Gonzalez-Dominguez, M. Lopez, I. Gonzalez-Garcia, O. Barca-Mayo, Protocol for ovariectomy and estradiol replacement in mice. *STAR Protoc.* **5**, 102910 (2024).
74. Z. Lin, S. Li, C. Feng, S. Yang, H. Wang, D. Ma, J. Zhang, M. Gou, D. Bu, T. Zhang, X. Kong, X. Wang, O. Sarig, Y. Ren, L. Dai, H. Liu, F. Li, Y. Hu, G. Padalon-Brauch, D. Vodo, F. Zhou, T. Chen, H. Deng, E. Sprecher, Y. Yang, X. Tan, Stabilizing mutations of KLHL24 ubiquitin ligase cause loss of keratin 14 and human skin fragility. *Nat. Genet.* **48**, 1508–1516 (2016).
75. Z. Pei, Y. He, J. C. Bean, Y. Yang, H. Liu, M. Yu, K. Yu, I. Hyseni, X. Cai, H. Liu, N. Qu, L. Tu, K. M. Conde, M. Wang, Y. Li, N. Yin, N. Zhang, J. Han, C. H. Potts, N. A. Scarcelli, Z. Yan, P. Xu,

Q. Wu, Y. He, Y. Xu, C. Wang, Gabra5 plays a sexually dimorphic role in POMC neuron activity and glucose balance. *Front. Endocrinol.* **13**, 889122 (2022).
76. L. Tu, J. C. Bean, Y. He, H. Liu, M. Yu, H. Liu, N. Zhang, N. Yin, J. Han, N. A. Scarcelli, K. M. Conde, M. Wang, Y. Li, B. Feng, P. Gao, Z. L. Cai, M. Fukuda, M. Xue, Q. Tong, Y. Yang, L. Liao, J. Xu, C. Wang, Y. He, Y. Xu, Anoctamin 4 channel currents activate glucose-inhibited neurons in the mouse ventromedial hypothalamus during hypoglycemia. *J. Clin. Invest.* **133**, e163391 (2023).
77. B. Feng, H. Liu, I. Mishra, C. Duerrschmid, P. Gao, P. Xu, C. Wang, Y. He, Asprosin promotes feeding through SK channel-dependent activation of AgRP neurons. *Sci. Adv.* **9**, eabq6718 (2023).
78. D. Y. Sanchez, A. L. Blatz, Block of neuronal fast chloride channels by internal tetraethylammonium ions. *J. Gen. Physiol.* **104**, 173–190 (1994).
79. G. Novarino, C. Fabrizi, R. Tonini, M. A. Denti, F. Malchiodi-Albedi, G. M. Lauro, B. Sacchetti, S. Paradisi, A. Ferroni, P. M. Curmi, S. N. Breit, M. Mazzanti, Involvement of the intracellular ion channel CLIC1 in microglia-mediated beta-amyloid-induced neurotoxicity. *J. Neurosci.* **24**, 5322–5330 (2004).
80. Y. He, P. Xu, C. Wang, Y. Xia, M. Yu, Y. Yang, K. Yu, X. Cai, N. Qu, K. Saito, J. Wang, I. Hyseni, M. Robertson, B. Piyarathna, M. Gao, S. A. Khan, F. Liu, R. Chen, C. Coarfa, Z. Zhao, Q. Tong, Z. Sun, Y. Xu, Estrogen receptor-alpha expressing neurons in the ventrolateral VMH regulate glucose balance. *Nat. Commun.* **11**, 2165 (2020).
81. M. J. Sanders, Z. S. Ali, B. D. Hegarty, R. Heath, M. A. Snowden, D. Carling, Defining the mechanism of activation of AMP-activated protein kinase by the small molecule A-769662, a member of the thienopyridone family. *J. Biol. Chem.* **282**, 32539–32548 (2007).
82. E. M. De Francesco, M. Pellegrino, M. F. Santolla, R. Lappano, E. Ricchio, S. Abonante, M. Maggiolini, GPER mediates activation of HIF1α/VEGF signaling by estrogens. *Cancer Res.* **74**, 4053–4064 (2014).
83. M. M. Ivanova, K. H. Luken, A. S. Zimmer, F. L. Lenzo, R. J. Smith, M. W. Arteel, T. J. Kollenberg, K. A. Mattingly, C. M. Klinge, Tamoxifen increases nuclear respiratory factor 1 transcription by activating estrogen receptor beta and AP-1 recruitment to adjacent promoter binding sites. *FASEB J.* **25**, 1402–1416 (2011).
84. H. Wan, Y. D. Yang, Q. Zhang, Y. H. Chen, X. M. Hu, Y. X. Huang, L. Shang, K. Xiong, VDAC1, as a downstream molecule of MLKL, participates in OGD/R-induced necroptosis by inducing mitochondrial damage. *Heliyon* **10**, e23426 (2024).
85. H. Ye, B. Feng, C. Wang, K. Saito, Y. Yang, L. Ibrahimi, S. Schaul, N. Patel, L. Saenz, P. Luo, P. Lai, V. Torres, M. Kota, D. Dixit, X. Cai, N. Qu, I. Hyseni, K. Yu, Y. Jiang, Q. Tong, Z. Sun, B. R. Arenkiel, Y. He, P. Xu, Y. Xu, An estrogen-sensitive hypothalamus-midbrain neural circuit controls thermogenesis and physical activity. *Sci. Adv.* **8**, eabk0185 (2022).
86. L. Zhu, Y. Yang, P. Xu, F. Zou, X. Yan, L. Liao, J. Xu, B. W. O'Malley, Y. Xu, Steroid receptor coactivator-1 mediates estrogenic actions to prevent body weight gain in female mice. *Endocrinology* **154**, 150–158 (2013).
87. C. Wang, Y. He, P. Xu, Y. Yang, K. Saito, Y. Xia, X. Yan, A. Hinton Jr., C. Yan, H. Ding, L. Yu, G. Shu, R. Gupta, Q. Wu, Q. Tong, W. R. Lagor, E. R. Flores, Y. Xu, TAp63 contributes to sexual dimorphism in POMC neuron functions and energy homeostasis. *Nat. Commun.* **9**, 1544 (2018).

Acknowledgments

Funding: Investigators involved in this work would like to acknowledge funding supports from the U.S. Department of Agriculture/Agricultural Research Service (CRIS3092-5-001-059 to Y.X.) and the Welch Foundation Q-2173-20230405 (to Z.W.). The work at INSERM U1297 U1048 was supported by the Institut National de la Santé et de la Recherche Médicale, CHU, Faculté de Santé—Médecine, Université de Toulouse III; the Agence Nationale de la Recherche (ANR-CE-14-0002/BENEFIT); and the INSERM and ANR (BENEFIT and NOSE4). **Author contributions:** M.Y. was involved in experimental design and most of procedures, data acquisition and analyses, and writing the manuscript. N.Y. performed the biochemical studies. B.F. and P.G. assisted in electrophysiology studies. K.Y. assisted in metabolic studies. Hesong Liu, Hailan Liu, Y.L., O.Z.G., K.M.C., M.W., X.F., L.T., J.C.B., Q.L., Y.D., Yuxue Yang, J.H., S.V.J., M.L.B., H.Z.W., and Yongjie Yang assisted in production of study mice and experiment procedures. J.F.A., P.G., and F.L. provided the ERα-C451A mutant mouse line and contributed to the study design, data interpretation, and manuscript writing. Z.W. provided the recombinant proteins and assisted in study design and data interpretation. S.G., B.R.A., Yang He and C.W. contributed to the study design, data interpretation and manuscript writing. Yanlin He and Y.X. were involved in study design and writing the manuscript, and they had full access to all the data in the study and took responsibility for the integrity of the data and the accuracy of the data analysis. **Competing interests:** The authors declare that they have no other competing interests. **Data and materials availability:** All data needed to evaluate the conclusions in the paper are present in the paper and/or the Supplementary Materials.

Submitted 5 March 2024
Accepted 26 August 2024
Published 2 October 2024
10.1126/sciadv.adp0696